Chapter 3

Aluminium Oxide Thin-Film based Biosensing Device

Chapter 3

Aluminium Oxide Thin-Film based Biosensing Device

3.1 Outline

The transparent thin film of the group III–VI based Al_2O_3 nanomaterial results in the better imaging for the adherent mammalian cells. Al_2O_3 is a metastable dielectric having wide bandgap of about ~6.7 eV at a room temperature and variable lattice structures with strong Al-O bonds [200]. Metastable polymorph structure of Al_2O_3 results in the various phase transition state at different temperatures such as γ, η, δ, θ and χ phase transition states, but thermodynamically α-Al_2O_3(corundum) transition phase is more stable than all the other phases [201]. Whereas the γ-Al_2O_3 transition phase has very fine particle size, hence it is used adsorbents, catalysts or catalysts supports, coatings and soft abrasives in industrial applications Moreover, the α-Al_2O_3 has high mechanical strength, hardness, high thermal conductivity, high corrosion, and abrasion resistance; hence it is used widely as electrical insulators, tunneling barriers, radiation-resistant materials, optical material in electronic and optoelectronic applications and as an alternative dielectric material in silicon-based devices. Since the α-Al_2O_3 has a high dielectric constant at least twice than that of silicon dioxide material, it is considered to be a suitable replacement for traditional used SiO_2 nowadays. When Al_2O_3 is annealed at a temperature below 400°C, it forms an amorphous structure with a different type of arrangements such as short-range order and long-range disorder [202].

On the other hand, Rajiv *et al*. [203] and Zhang *et al.*[204] have reported that the Al_2O_3 nanoparticle is more biocompatible material i.e., the Al_2O_3 nanoparticle has shown lesser cytotoxicity than that of Zinc oxide, Titanium dioxide, silicon dioxide, Ferric chloride, and Cobalt tetraoxide. Generally, the Al_2O_3 nanomaterial is used as a layer on the surface to increase resistance towards abrasion [205]. Hence, the focus of this work is on determining the influence of Al_2O_3 nanomaterial's surface properties on protein adsorption and subsequent cell adhesion and proliferation, as in the *in vitro* cell-substrate interaction studies. The nanomaterial's surface properties generally show its strong impact on cellular behaviour such as adhesion rate, cell morphology and extent of spreading and proliferation. Whereas, the adhesion of cells to extracellular matrix (ECM) proteins adsorbed onto implant surfaces is particularly essential to establish host responses in biomaterial and tissue-engineering applications [206], [207]. To the best of our knowledge, none of the work have reported so far on fabricating Al_2O_3 thin film nanomaterial-based biosensing platforms to determine the status (functional and behavioural information) of adherent cell when cultured in vitro. Furthermore, Al_2O_3 nanomaterial's thin film can be either easily modified or immobilized with a variety of chemical groups, functional peptides and macromolecules to form complexes; revealing their potential application as a coating material to functionalize the surface of any biomechanical device.

3.2 Materials and methods

3.2.1 Materials

C2C12 Mouse Myoblast cell linewas received from NCCS, Pune, India. Dulbecco's Modified Eagle Medium (DMEM) high glucose, Fetal bovine serum (FBS), penicillin-streptomycin (100 µg/mL penicillin and streptomycin) and gelatin type B (cell culture tested) were received from HiMedia India. Phosphate buffered saline (PBS, 10X) and Ultrapure Al_2O_3 powder (99.99%) were received from Sigma (Merck) India. High temperature Teflon adhesive tape and single-side indium tin oxide (ITO) coated glass substrate (7 × 7 inch, ITO thickness = 150 nm) were procured from local vender.

3.2.2 Fabrication of MIM biosensor

ITO coated glass substrate of 25 × 15 mm^2 (Figure 3.1a) was covered using Teflon tape and patterned to get an electrode dimension of 12 × 5 mm^2 at each side with a gap of 1 ± 0.2 mm (at center) as in Figure 3.1b. The uncovered ITO regions were etched-out to get a co-planar electrode system as shown in Figure 3.1c using 9 M Hydrochloric acid (HCl, 37%, Merck India) [14], [15]. Then, the patterned ITO coated glass substrates were thoroughly cleaned using standard wet chemical cleaning procedures. On the other side, ultrapure Al_2O_3 powder (99.99%) was mixed with a binder, and pressed into a pellet. The pellet was heated for 3 h at 1200 °C in the ambient air atmosphere to decompose the binder. Then, the heated Al_2O_3 pellet was used as the source material in the electron beam evaporation (EBE) unit (HINDVAC, Bangalore, India; Model No. FL400 SMART COAT 3.0 A). The Al_2O_3 pellets were vaporized on the cleaned patterned substrates at a deposition rate of ~5.00 Å/s to get a film of thickness ~100 nm in the EBE unit [208], [209]. The shadow masking technique is used to deposit the Al_2O_3 in the desired shape and size as shown in Figure 3.1d. The deposition rate and thickness of the film were monitored using the in-built digital thickness monitoring module (SQM-160, INFICON). Later, the obtained Al_2O_3 coated patterned ITO samples were annealed at 400°C in the inert Argon gas atmosphere with about ~30 sccm gas flow for 1 h in the muffle furnace to obtain crystallized Al_2O_3 thin film [210], [211]. A custom-designed polypropylene well was attached to the top of the substrates coated with Al_2O_3 thin film for maintaining the culture media. The customized-well was sealed using polydimethylsiloxane (PDMS) (Dow Corning, Sylgard 184) to avoid the leakage of culture media [9]. We have mentioned this cell culturing device as the fabricated cell-device, as shown in Figure 3.1e.

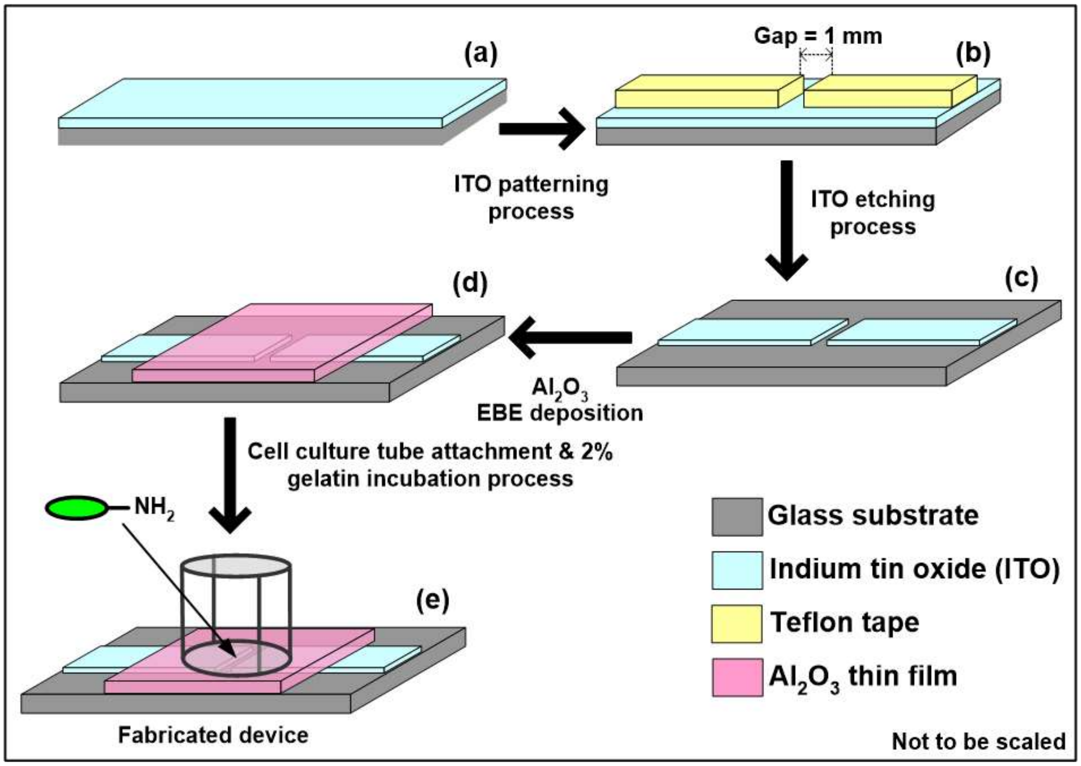

Figure 3.1: Fabrication process of EBE deposition Al_2O_3 thin-film based biosensing device.

3.2.3 Cell culture procedure

Mouse myoblast C2C12 cells were used in gelatin coated Al_2O_3 platforms. The cells were seeded at a density of 4,000 cells/well for the analysis. The cell culture medium was changed before every observation. Ref **Section 2.2.3** for more detailed cell culture procedure. The cell study was done in triplicate (n = 3), and its average result was represented.

3.3 Results and discussion

To analyze the effect induced by cellular functional behaviour which alters the characteristic electrical properties, we seeded cells of 4000 cells/well concentration to the fabricated device. The change in the characteristic electrical properties was determined in terms of change in resistance, capacitance or impedance developed correspondingly with a change in the morphology of the cells adhered to the surface over the time period. In Figure 3.2a, it was observed that myoblast cells became flat, which implied that the cells started to grow on the underlying surface, as it adapted to that micro-environmental condition surrounding them. From the microscopic image, a significant change in the morphology of myoblast cells was observed as shown in Figure 3.2a-d. The experiments were carried out at different time intervals to avoid contamination and other adverse effects on the developed microenvironment.

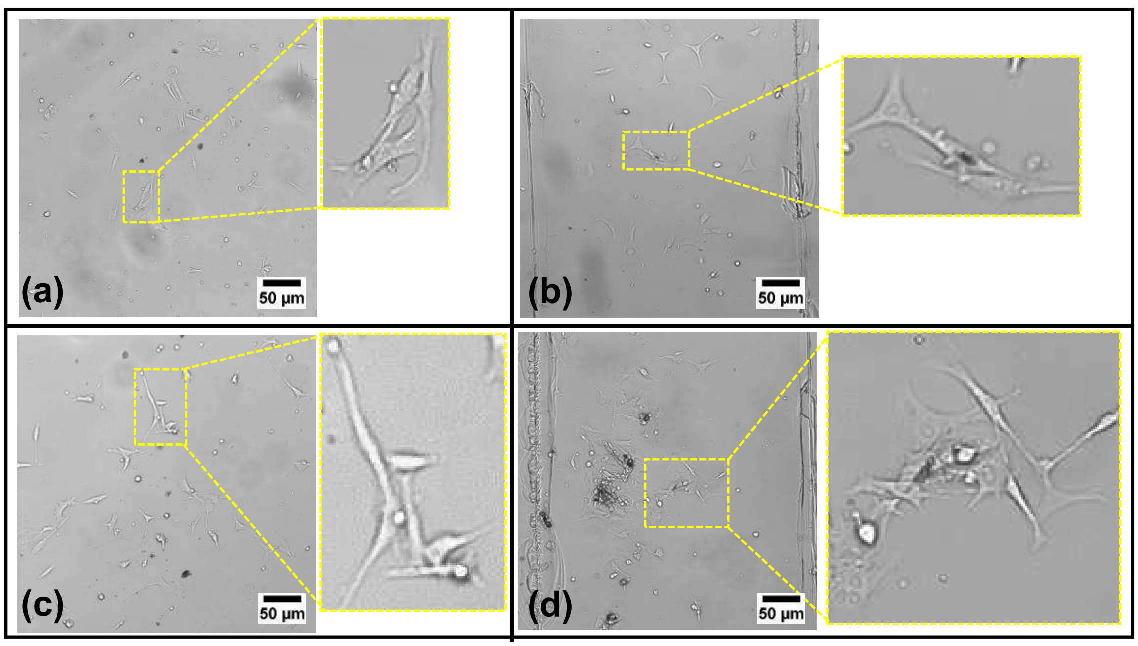

Figure 3.2: Morphology of C2C12 cells at various time intervals: (a) 8 h, (b) 24 h, (c) 48 h, and (d) 72 h; Scale bar: 50 µm.

Generally, the outer environment of the cell is comparatively positive than the inner side of the cell. The potential difference across the cell is maintained due to the various physiological processes exhibited across the cell membrane to govern and perform the biological cell's basic functionality. When the C2C12 cells were seeded to the fabricated device, they gradually drifted downwards to settle on the substrate. They started adhering to the surface of the fabricated device; due to which the active sensing area available for free-flow of current gets changed and alternatively the corresponding characteristic electrical properties of the fabricated device also get altered. Further, the electrical properties of the biological cells were considered to be varied as a function of frequency. In brief, at a lower frequency (< 1 kHz) the depth of penetration of an AC signal is very less across the cell-membrane; hence the more current flows in the extracellular region than that of the intracellular region of the biological cells as a function of frequency and it is termed as the 'α' dispersion, which is associated phenomena of ion diffusion exhibited across the membrane. Wherein, at mid-frequency (1 kHz – 100 kHz), the depth of penetration of an AC signal is more than the 'α' dispersion; hence the more current flows in the extracellular region while comparatively less current flows through the cell membrane into the intracellular region due to which a polarization effect or Maxwell-Wagner phenomena developed across the cell-membrane as a function of frequency and it is termed as the 'β' dispersion. At higher frequency (>100 kHz), the water molecules present in that biological medium gets polarized due to which more current flows in the intracellular region than of the extracellular region of the biological cells as a function of frequency and it is termed as the 'γ' dispersion [8], [79]. Thus, to analyze the frequency dominated changes – capacitance, the magnitude of impedance and phase of impedance *vs.* frequency plot were recorded and correlated with the microscopic images. The results revealed that the capacitance gets decreased with an increase in the magnitude of impedance and vice-versa, correspondingly with the progression of function of cells such as adhesion, proliferation and differentiation, as shown in Figure 3.3a and Figure 3.3b. Moreover, it is also observed that a change in the shape of cells i.e., morphological change, affects the phase of impedance correspondingly [192], as shown in Figure 3.3c. Further, from the Nyquist plot, it was revealed that the shift in the real *vs.* imaginary impedance data (shown in Figure 3.3d) is due to the progression of cellular functional behaviour on the surface of the substrate.

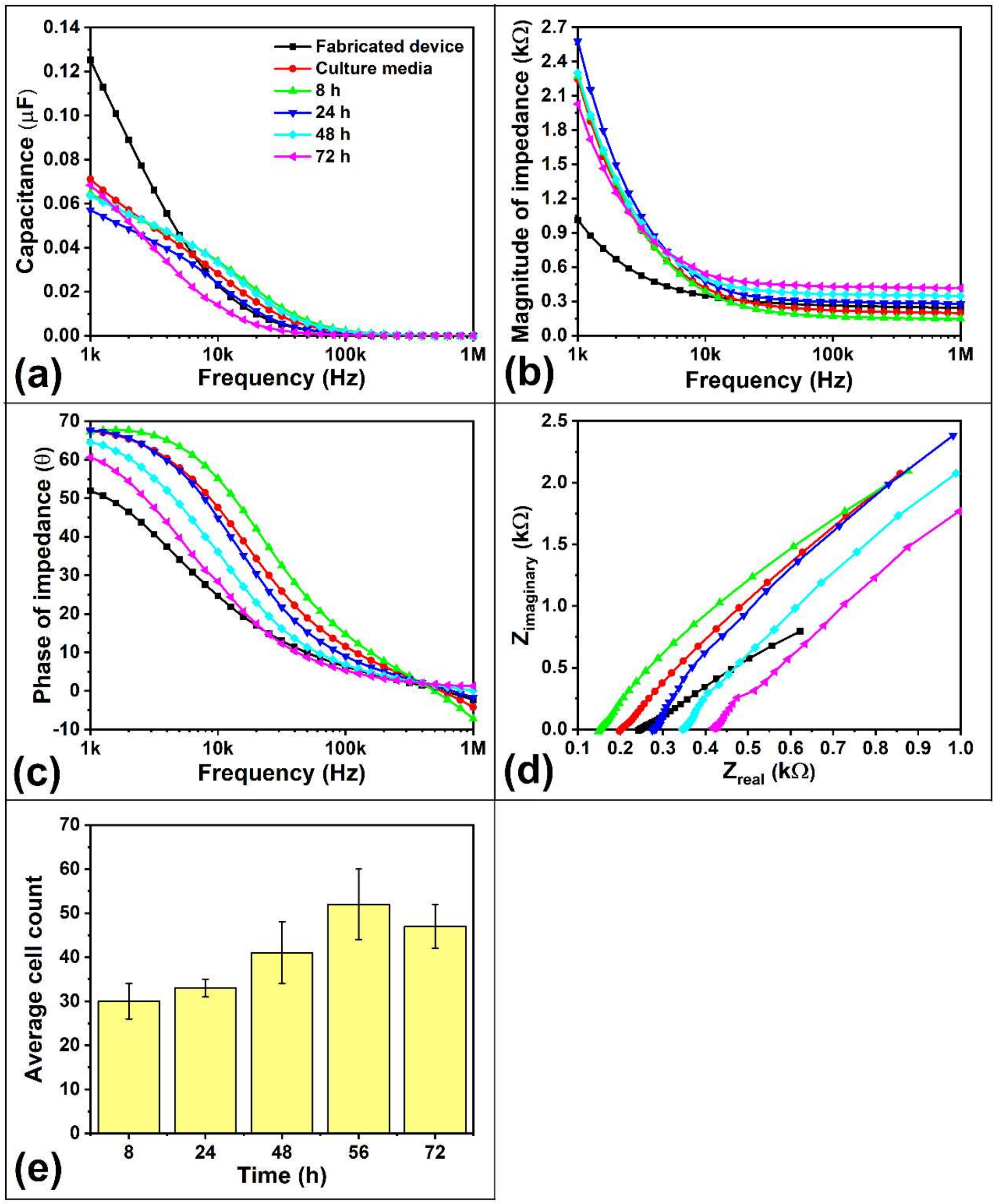

Figure 3.3: Changes in the characteristic electrical properties of the Al_2O_3 thin film due to dynamic behaviour of myoblast cells in culture: (a) capacitance *vs*. frequency plot, (b) magnitude of impedance plot, (c) phase of impedance plot, (d) Nyquist plot and (e) Average cell count at different time point.

The magnitude of impedance data was used to fit the equivalent electrical model to calculate the theoretical relationship between the surface-electrolyte-cell interface in the presence of biological cells [181]. Figure 3.4 shows the equivalent electrical model used in the work and Table 3.1 shows the corresponding model parameters of the equivalent electrical model used. The equivalent electrical model was separated into a device component and tissue component to represent fabricated devices containing biological cells. The fabricated device was represented with an RC circuit having a resistor (R_s) in series with a resistor (R_p) and capacitor (C_p) in parallel, as in Figure 3.4a. Generally, the insulating property of cell membrane (C) is represented by the biological cell's membrane resistance (R_m) and capacitance (C_m). Hence, the tissue or cell component was represented with a resistor (R_m) and capacitor (C_m) in parallel combination.

Upon excitation, the current flows from the ITO electrode and the interfacing region. The interfacing region contains Al_2O_3 thin film and the biological medium i.e., the biological cells and the cell culture medium on its surface through which the transfer of electrons take place. However, the capacitance developed by the biological cells and cell growth are more dominating than the device capacitance. Hence, the device's capacitor (C_p) was replaced with the tissue component to represent the charged double-layer developed across the fabricated cell-device (surface)-electrolyte-cell interface. The developed charged double-layered interface is due to the biological medium; hence it is directly related to a capacitor (C_{dl}) in parallel with a resistor (R_{dl}), which together represented by a Constant Phase Element (CPE) with an empirical parameter 'n' ($0 \leq n \leq 1$) to represent the tissue component [79]. If n = 1, then the fabricated cell-device act as an ideal capacitor; whereas if n = 0, then the fabricated cell-device acts as an ideal resistor and the impedance of CPE (Z_{CPE}) can be calculated by an equation 3.1.

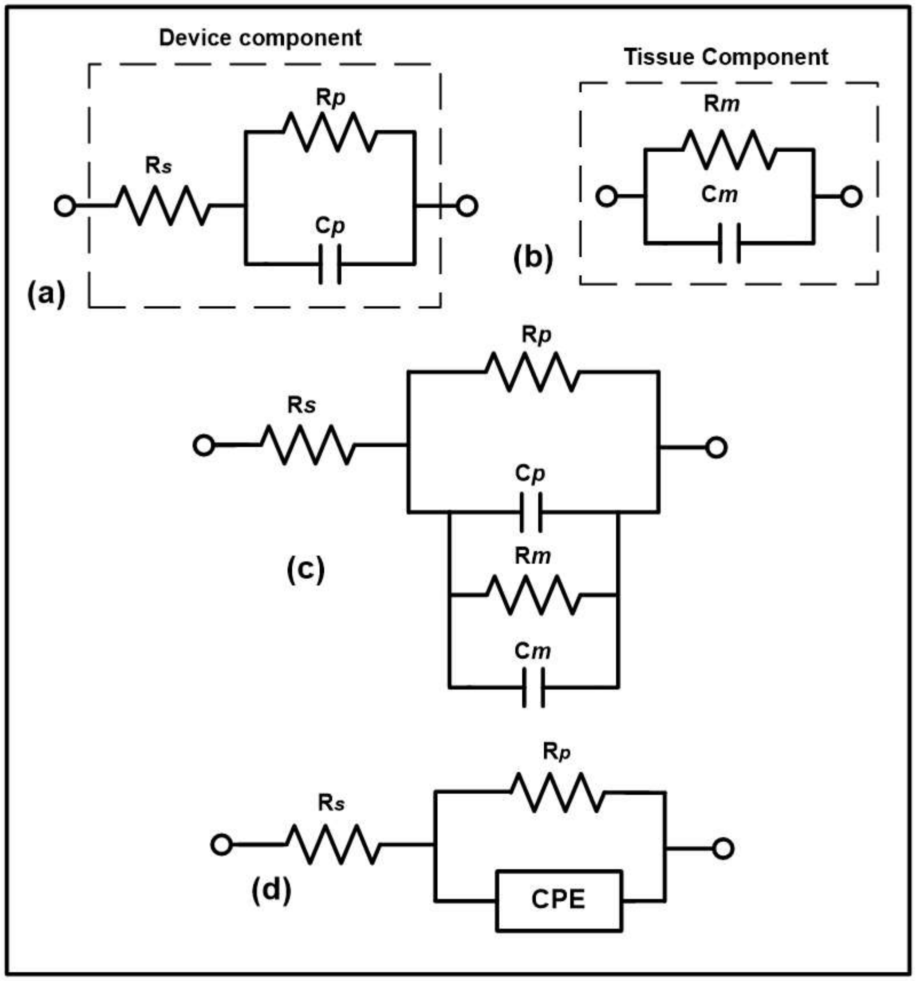

Figure 3.4: Equivalent electrical circuit model to represent the surface-electrode-cell interface: (a) fabricated device component, (b) tissue component, (c) fabricated device with tissue component and (d) cell-device.

$$Z_{CPE} = \frac{1}{(j\omega)^n \times Q_p} \tag{3.1}$$

The equivalent electrical circuit model of the fabricated device ($Z_{Fabricated\ device}$) can be represented by equation 3.2:

$$Z_{\text{cell-device}}(\omega) = \left[R_s + \left(X_{C_p} \parallel R_p \right) \right] \tag{3.2}$$

Where, the $Z_{tissue\ component}$ can be represented as in equation 3.3

$$Z_{tissue\ component}(\omega) = \left[R_m \| C_m\right] \tag{3.3}$$

Hence, replace $Z_{tissue\ component}$ in $Z_{cell-device}$ as in equation 3.4

$$Z_{\text{cell-device}}(\omega) = \left[R_s + \left(\left[R_m \| C_m\right] \| R_p\right)\right] \tag{3.4}$$

To represent the charged double-layered interface developed due to biological medium, the equation 3.4 is replace with Z_{CPE} to get equation 3.5

$$Z_{\text{cell-device}}(\omega) = \left[R_s + \left(Z_{CPE_t} \| R_p\right)\right] \tag{3.5}$$

Simplifying equation 3.5, the $Z_{cell-device}$ becomes equation 3.6

$$Z_{\text{cell-device}}(\omega) = \frac{R_s + R_p}{1 + \left[\left((j\omega)^n Q_p\right) \times R_p\right]} \tag{3.6}$$

Here in this work, the measured impedance data was fitted using Non-Linear Least Mean Curve Fitting Method [8] to analyze the change in the progression of cellular functional behavior in terms of EEC model parameters extracted using equation 3.6.

The EEC model parameters were given in Table 3.1. The result reveals that the resistance (R_s) and the reactance (Q_p) of Z_{CPE} tissue component get increased with a decrease in resistance (R_p) and empirical parameter (n). Thus, change in concentration of the biological cell on the surface modulates the model parameters accordingly to divulge the dynamic behaviour of the biological system. Further, to visualize the change in average cell count over the time of period, a separate figure containing the average cell count *vs.* time plot is given (as shown in Figure 3.3e). From the outcomes, it is concluded that the change in the characteristic electrical properties of the fabricated device is highly influenced by the progression of cellular processes exhibited by the myoblast cells.

Table 3.1: Calculated EEC model parameters.

Model Parameters	**Fabricated device**	**Culture medium**	**8 h**	**24 h**	**48 h**	**72 h**
n	--	0.832	0.824	0.859	0.843	0.821
Q_p (F)	(C_p) 12.98×10^6	31.39×10^6	33.03×10^6	21.70×10^6	28.41×10^6	40.57×10^6
R_p (Ω)	928.12	7.60×10^5	6.80×10^5	5.07×10^5	4.23×10^5	2.75×10^5
R_s (Ω)	271.02	200.73	136.36	269.54	338.37	407.43
R^2	0.992	0.999	0.999	0.999	0.999	0.999

3.4 Conclusion

In the present work, we have demonstrated that the dynamic behaviour of myoblast cells is capable of altering the typical, predefined characteristic electrical behaviour of the fabricated *in vitro* cell-substrate sensing devices. Further, the proposed device is working significantly to determine various cellular functions such as cell adhesion, spreading, proliferation, and differentiation. The effect induced by cellular functional behaviour is well correlated with both changes in the characteristic electrical property and microscopic observation of the cells as well with an equivalent electrical model used. Hence, the proposed device could be used for various biosensing applications wherein dynamic changes of the biological cells play a vital role and need to be essentially examined.